

Martensitic transformation and related properties of $\text{Fe}_{69.4}\text{Pd}_{30.6}$ ferromagnetic shape memory ribbons

F. TOLEA, M. SOFRONIE*

National Institute of Materials Physics, P.O. Box MG-7, 077125, Magurele-Bucharest, Romania

Ferromagnetic shape memory alloys (FSMA) have attained strong interest over the last years and Fe-Pd alloys seems to be more suited for engineering and medical applications, due to their improved ductility and biocompatibility compared to the well-known Ni_2MnGa alloy. The shape memory effect in disordered Fe-Pd (30 at.% Pd) is associated with FCC-FCT thermoelastic martensitic transformation. The melt-spinning technique enables to get ribbons with the FCC meta-stable structure preventing the precipitation of undesirable BCT irreversible phase and subsequent proper thermal treatments could improve the characteristic parameters of the martensitic transformation. The present work reports the effect of the rapid solidification (via melt-spinning technique) and the different thermal treatments on the microstructure, martensitic transformation and magnetic properties of the $\text{Fe}_{69.4}\text{Pd}_{30.6}$ ribbons. The samples were investigated by calorimetry, X-ray diffractometry, scanning electron microscopy and magnetometry. Two different structures induced by the distinct thermal treatments and responsible for the characteristic behavior of the martensitic transformation, were noticed and discussed in details. The high temperature treatment for short time stabilized the FCC phase and slightly decrease the martensitic transformation temperature, while the annealing at low temperature for longer time promotes the reduction of the amount of transforming FCC phase by its partial decomposition in the stable phases, causing the fall of the heat of transformation.

(Received May 24, 2018; accepted November 29, 2018)

Keywords: $\text{Fe}_{69.4}\text{Pd}_{30.6}$ alloy, Ferromagnetic shape memory ribbons, Martensitic transformation, Magnetic properties

1. Introduction

With around 30 at.% Pd, the Fe-Pd alloy is a Ferromagnetic Shape Memory Alloy (FSMA) because these undergo the martensitic transformation (MT) - a thermo-elastic and diffusion-less phase transformation between two magnetically ordered phases. On cooling, the high temperature austenite phase with face centered cubic (FCC) structure turns to the low temperature martensite phase, with face centered tetragonal (FCT) structure. The MT temperature (lower than the Curie temperature of the austenite phase) is very sensitive to the alloy composition and for this peculiar alloy is around the room temperature. By slightly decreasing the Pd concentration, the thermo-elastic transformation observed at lower temperatures is either followed or accompanied by a nonthermo-elastic one, i.e. the transition FCC-BCT, where BCT is a body centered tetragonal structure. This last mentioned nonthermo-elastic transformation weakens the shape memory effect and has to be avoided. The phase diagram, the martensite transformations [1], the magnetic properties [2], magneto-anisotropy [3] and magneto-elastic properties of Fe-Pd alloys have been studied since more than three decades, but the interest was renewed in the last years, after the report of a giant magnetostriction of 0.6% achieved in a $\text{Fe}_{70}\text{Pd}_{30}$ -single crystal [4]. Due to this effect, known as magnetic field-induced strain (MFIS), new intensive studies were devoted to the FSM behavior of $\text{Fe}_{70}\text{Pd}_{30}$ alloy, as a single crystal [5]. T. Wada et al. [6] studied the influence of the magnetic field on the martensite structure of a Fe-30.5 at.% Pd polycrystal

concluding that, in martensite, the magnetization process is mainly achieved by rotation of magnetization direction rather than by moving magnetic domain walls. K. Seki et al. [7] discussed the influence of grain size in sintered $\text{Fe}_{70}\text{Pd}_{30}$ alloy (from nanometers to several micrometers) on both the martensite transformation temperature and transformation mechanism. In order to stabilize the FCT martensite and to avoid the formation of the undesirable BCT martensite, the addition of a third alloying element (Ni, Pt, Co, Mn) was used [8-13].

While the FCC-phase responsible for the shape memory effect (SME) in Fe-Pd is stable only at high temperature, it becomes generally instable, as a single phase, in a bulk material prepared by classical methods. There is a way to obtain ribbons with a non-equilibrium structure, in which the high temperature FCC structure can be frozen as a single phase, namely rapid solidification via melt-spinning technique. Expectedly, the ferromagnetic SME obtained on ribbons prepared by this method, should be lower than in case of single crystals, because the variant strains will cancel reciprocally. However, the other structural and magnetic characteristics of MT can be successfully studied on FCC - single phase ribbons. Prior research on Fe-Pd ribbons discusses the MT [14,15], the variation of the magnetic properties in correlation with the process of FCC phase decomposition [16], the effect of spinning wheel velocity on phase composition and microstructure [17] and the thermo-mechanical properties [18].

This work reports a detailed study on how the martensitic transformation is reflected in the evolution of

magnetic properties of the as-quenched and annealed melt-spun ribbons with composition $\text{Fe}_{69.4}\text{Pd}_{30.6}$.

2. Experimental

The alloy ingot was prepared by arc melting under argon protective atmosphere, starting from high purity elements and obtaining a bulk alloy with nominal composition $\text{Fe}_{69.4}\text{Pd}_{30.6}$. Subsequently, it was cooled ultrafast via melt spinning technique. Long rapidly quenched ribbons of about 30 μm thickness and 3 mm wideness were obtained at a copper wheel velocity of 20 m/s, applying 50 kPa argon overpressure; the diameter of the nozzle aperture was 0.5 mm. The as-quenched ribbons (denoted as A0) were subsequently thermally treated in vacuum quartz ampoules for 60 minutes at 770 K, resulting samples A1 and respectively for 15 minutes at 1220 K (sample denoted A2). Each treatment was followed by a direct quenching of the sample in ice water. X-ray diffraction (XRD) using a Seifert diffractometer (using $\text{Cu K}\alpha$ radiation) was performed for structural investigations. The surface morphology and the chemical composition of the ribbons were examined by Scanning Electron Microscopy (SEM) and Energy Dispersive X-ray Spectroscopy (EDS) in a Zeiss Evo 50 XVP microscope, respectively. The martensitic transformation temperatures and the transformation heat were determined using a differential scanning calorimeter (DSC) model 204F1Phoenix-Netzsch (with a scanning rate of 20 K/min). Magnetic measurements were performed by SQUID (Quantum Design) magnetometer, for temperatures below 350 K, whereas for high temperature thermomagnetic measurements, the vibration sample magnetometry option of a Physical Property Measurement System (Quantum Design) was used.

3. Results and discussions

3.1. Structure characterization

The room temperature X-ray diffraction patterns collected on samples A0, A1 and A2, the last two obtained via different thermal treatments are shown in Fig. 1. The as quenched ribbons (A0) exhibit a unique single FCC phase (the high temperature stable phase), obtained in the ribbons due to the rapid cooling, specific for the melt spinning technique. In order to eliminate the quenched-in tensions and to refine the crystalline structure, thermal treatments were performed; these have had different effects, depending on the annealing temperatures.

Thus, a temperature of heat treatment slightly lower than the decomposition temperature initiates the transformation of the non-equilibrium disordered FCC phase into the equilibrium phases, namely the BCC iron based one and the quasi equiatomic Fe-Pd with L1_0 structure. This phenomenon occurs after the thermal treatment carried out at 770 K- see sample denoted A1. After the treatment at high temperature (1220 K) and

subsequent quenching, no other phases were observed in sample A2, excepting FCC austenite.

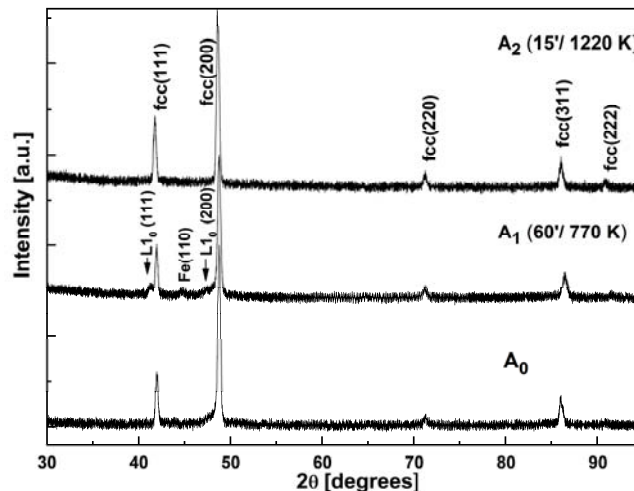


Fig. 1. Room temperature XRD patterns of as quenched ribbons (A0) and after thermal treatments at 770 K (A1) and 1220 K (A2)

A slight increase of the lattice constant from 0.373 nm, as determined for the as prepared ribbons, to 0.375 nm, reflects the structural refinement. Another feature induced by the processing route is the high texture of the ribbons. It is worth noting that, in the measurements presented in Fig. 1, the free sides were exposed to the X rays and not the sides in direct contact to the wheel surface during the melt spinning process. For a non-textured polycrystalline sample with FCC structure, the most intense peak belongs to the (111) reflection plane, followed by the peak belonging to the (200) reflection plane, whose intensity is about 40% less. However, the XRD patterns recorded from the free surface of the as prepared and the annealed ribbons exhibit the highest reflection corresponding to the (200) plane. Such a texture often appears in rapidly quenched alloys with cubic structure, showing that the cubic plane (100) develops preferentially at the free surface of the ribbon when a microstructure with columnar grains is developed [19,20]. The same type of texture, although not so evident, is observed on the other side of the ribbons (the one in contact to the wheel).

The SEM images, of the free (Fig. 2(a)) and in contact to the wheel (Fig. 2(b)) sides, of as quenched ribbons (sample A0) point to a large difference between the grains size of the two ribbons sides, reflecting the higher cooling rate on the wheel side as compared to the free one. On the wheel side, the grains are contacting each other, have wavy boundaries and their mean size is 2-3 μm . On contrary, the grains on the free side are larger (5-7 μm) with no contact between them and with almost regular boundaries, suggesting a columnar microstructure of the sample. Also, martensitic variants are visible on some grains, mainly on the largest ones from the free ribbon side. After the thermal treatment at 1220 K, the grains size increases, especially on the contact to the wheel side, also the grains size dispersion inside the ribbons is reduced

(Fig.2(c) and (d)). On the both sides, the grains are contacting each other, with smooth interfaces and the effective volume of grain boundaries is lowered. The small

blisters observed are generated by the diffusion of the gas previously dissolved in the melt during the preparation.

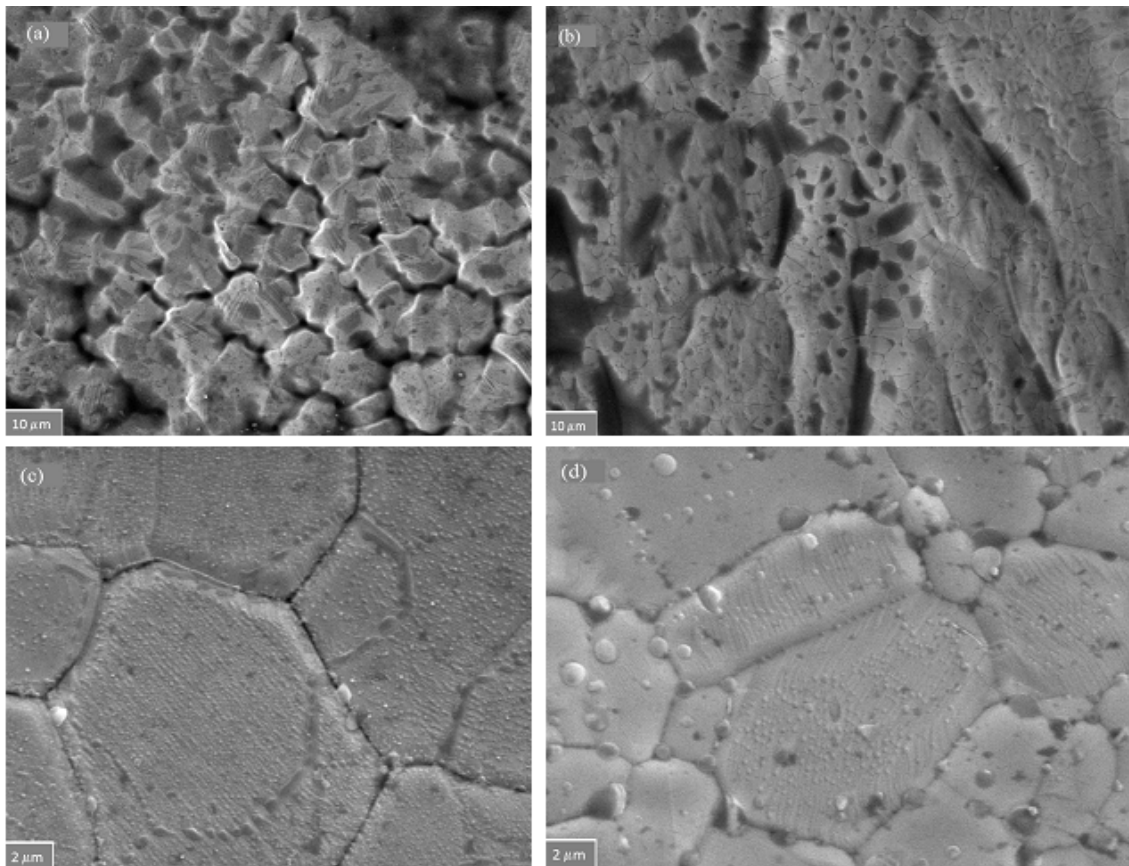


Fig. 2. The SEM images: (a) the free and (b) in contact to the wheel sides of as prepared ribbons (sample A0), (c) after the heat treatment of 15 minutes at 1220K (sample A2) for the free side and (d) contact side

3.2. Thermal characterization of the martensitic transformation

Thermal analysis of the studied samples highlights the characteristic temperatures of the MT: Martensite start (Ms) and finish (Mf), Austenite start (As) and finish, (Af) and the heat of transformation (Q), thermal hysteresis (Af-Ms) and MT range (Af-Mf). A first DSC scan was performed on all samples, in a large temperature range (80K - 400K). It is worth mentioning, no evidence for any irreversible transformation was found, only the thermo-elastic transformation, near room temperature. The specific parameters of the MT have been established after a second scan, performed only in the temperature range of interest (Fig. 3.). Using the tangential line method, the transformation temperatures were determined and the heat of transformation, Q, was calculated via the Netsch software. The A0 as quenched ribbons exhibit a relative low value for Q (0.22 J/g) and very broad peaks for MT, reflecting a transformation which occurs gradual and slow, extended over a large temperature interval between 293K martensite start (Ms) and 270K martensite finish (Mf)

temperatures. Additionally, the MT characteristic temperature range (Af-Mf) is about 30 K.

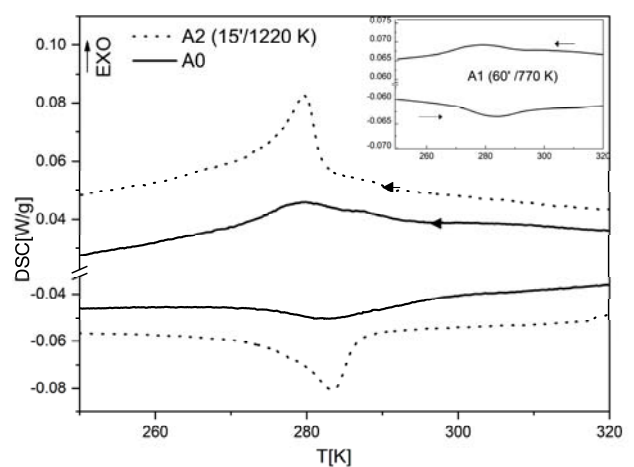


Fig.3. The DSC curves for as prepared sample A0 and after different thermal treatments (A1(Inset) and A2)

The MT temperature range for A1 sample is not changed after the thermal treatment performed at 770 K, but the heat of transformation is drastically reduced (Inset Fig.3) and the characteristic temperatures become $M_s=289\text{K}$, $M_f=263\text{K}$, $A_s=268\text{K}$, $A_f=294\text{K}$. Here it is to note that, even below the martensite finish temperature, the tetragonal distortion continues to increase (e.g. as suggested by magnetic measurements presented in the followings), so that the transformation can be labeled as “a weak first-order” one. Concerning the heat of transformation, it is to note that the highest Q value obtained on actual ribbons is 2.5 times smaller than that of a single crystal [5] and approximately 1.2 smaller than that reported for similar bulk samples with the same composition [7,21].

The A2 ribbons, annealed at 1220 K exhibit sharper MT peaks and a narrower characteristic temperature range of the MT (~ 13 K), while Q reaches the highest value among the analyzed samples (0.59 J/g). The characteristic temperatures of MT for A2 sample are: $M_s=280\text{K}$ and $M_f=274\text{K}$, $A_s=277\text{K}$ and $A_f=287\text{K}$. It is worth mentioning that the heat of transformation in Fe-Pd alloys is one order of magnitude smaller than for other shape memory alloys, being generally attributed to the low degree of lattice distortion at the transition temperature.

In DSC measurements, the peak area, representing the heat of transformation, is given by the chemical enthalpy variation (latent heat) as the main contribution, to which are added the secondary non-chemical energy terms for the stored elastic strain energy at the nucleation of martensite and the dissipated energy due to internal resistance to phase boundary movement. The chemical enthalpy variation is determined essentially by the lattice change and there are no reasons to consider different c/a variations in ribbons, poly-crystals or single crystals with similar structure. Hence, the non-chemical energy terms are responsible for different reported Q values. By decreasing the crystal grain size, the mentioned non-chemical energy terms are enhanced and additional energy is needed to initiate transformation [22] which is reflected in the decrease of M_s . Accordingly, the MT might not occur below a critical grain size [7,23]. Furthermore, an important increase in the stored elastic strain energy is due to the occurrence, in the small grains, of the single variant transformation [7] in contrast to the multi variants mode, characteristic for the large grains, where strain is reduced by the self-accommodation of variants. Thus, the relatively lower Q value obtained for A0 ribbons (0.22 J/g) as compared to 0.52 J/g for the heat of transformation for sample A2, may be assigned to the large stored elastic energy in the small grains; additionally, for small grains, a decrease of the martensite start temperature would be expected, but, the quenched-in strains stored in ribbons during the processing route have opposite effect, so that the final consequence is just the broadening of the MT. The heat treatment at 1220 K (sample A2) improves

homogenization, refines the crystalline structure by stabilizing the FCC phase, reduces the grains size differences, decreases the boundaries volume (see Fig. 2. (a) and (c)) and relaxes the quenched-in strains enlarging so the overall Q value, as compared to the case of A0 sample.

On the other side, the relatively low Q value (0.05 J/g) observed for A1 ribbons annealed at 770 K (two phases), may be attributed to the reduction of the amount of transforming FCC phase by its partial decomposition in the stable phases, as evidenced by also the X-ray measurements. For example, a similar low Q value (~ 0.03 J/g) was reported on as prepared ribbons containing a small amount of non transforming BCT phase, in addition to the FCC active phase [17].

3.3. Magnetic properties

The thermo-magnetic measurements performed for the high temperature range (in an applied field of 200 Oe) on A0 ribbons (Fig.4(a)) show an order-disorder magnetic transition near 570K, clearly belonging to the FCC phase, attested by room temperature X-ray diffraction data. The relative wide temperature range of magnetization decay reflects a defective structure with vacancies and quench-in strains responsible also for the broad and dulled MT peak of DSC data. Furtherheating, at temperatures exceeding 870 K, induces decomposition in two stable phases, as evidenced by subsequent magnetization measurements performed during the cooling procedure. According to Fig. 4 (a), the cooling branch of magnetization confirms the presence of the body centered cubic (BCC) structure of metallic iron having ordering temperature near 1040 K and of the $L1_0$ phase with $T_c=720$ K. A very slight jump of magnetization is also observed at about 580 K, standing for a rest of the austenite FCC phase, which bears the magnetic order-disorder transition. Fig.4(b) presents the thermo-magnetic measurements realized on ribbons A2 (heat treated 15 minutes at 1220 K and then rapidly quenched). A first thermo-magnetic loop was done up to 850 K and a second one up to 1000 K. The behavior is completely reversible along the first cycle (represented by dotted line in Fig. 4 (b)). In comparison to the as prepared ribbons, the magnetization decrease at the Curie temperature of the austenite phase (590 K) is sharper, denoting a more ordered structure.

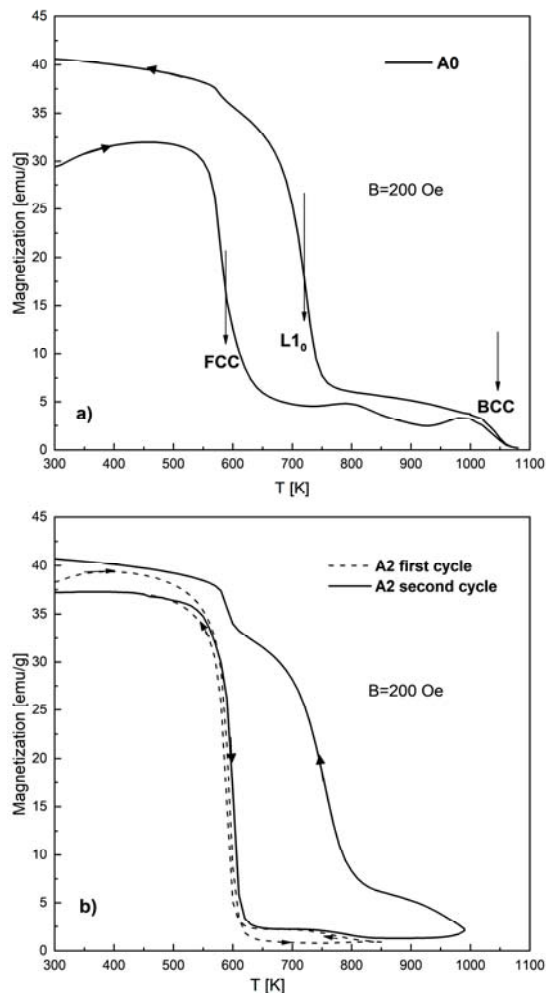


Fig. 4. Thermo-magnetic measurements performed in low magnetic field (200 Oe) on (a) as prepared ribbons and (b) on ribbons thermal treated 15 minutes at 1220 K

Referring to the second cycle, the decomposition of the FCC phase begins above 870 K and a similar irreversible behavior occurs, as for sample A0 (as prepared ribbons). However, the heating/cooling velocity (of 5 deg/min) was not slow enough for complete phase decomposition in sample A2 and a step at about 600 K is evidenced. Being more pronounced than in sample A0, this step proves the persistence of a relatively higher amount of FCC phase. It was reported that for as prepared ribbons, of similar composition as the analyzed ones, the complete decomposition was obtained after 2 hours of heat treatment at 770 K even if, the structure refinement of the two stable phases requires a much longer heat treatment [16].

The thermo-magnetic measurements performed over the temperature range of MT in FSMA, are very useful instruments for studying the distinct feature of the structural transition in correlation with the magnetic behavior [8], [21], [24-26]. Fig. 5 exhibits the thermo-magnetic scans for sample A2 measured at temperatures lower than 350 K, under different constant magnetic fields.

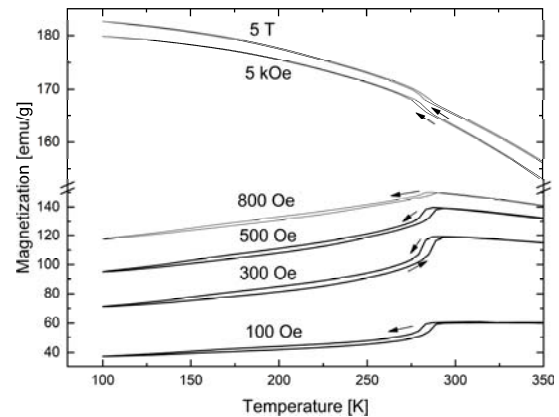


Fig. 5. The thermo-magnetic scans for sample A2 performed at temperatures lower than 350 K, under different constant magnetic fields

These measurements were realized by cooling down the sample from 350 K to 100 K and then warming it up. In this temperature range, the data reflect only the FCC-FCT thermo-elastic transformation with a large thermo-magnetic hysteresis.

By cooling the sample in relative low magnetic fields (≤ 800 Oe), an abrupt decrease of magnetization occurs at the martensite start temperature, but no evidence for a real finish transformation temperature is provided, since the magnetization continues to decrease continuously, noticeable much slowly. Looking on the increasing temperature branch, the magnetization enhances gradually up to the austenite finish temperature. A thermo-magnetic hysteresis in the range of MT is common for all FSMA [8], [21], [25], being a characteristic fingerprint for the first order phase transitions. The tangent method (intersection of the tangent to the fastest variation of magnetization with quasi-saturated branches), may provide information on all the involved transition temperatures, and might be considered as an alternative to DSC measurements. Nevertheless, magnetization measurements are able to support the continuous structural change at low temperatures. Concerning the measurements in low magnetic fields, the sharp decrease of magnetization during the cooling process is associated to the increase of the magneto-crystalline anisotropy induced by the structural transformation from cubic to tetragonal structure. It is also well known that for the Fe-Pd alloys, the tetragonal distortion continues to evolve even below the martensite finish temperature [5], [27], giving rise to the large thermal hysteresis evidenced by our measurements (e.g. no overlapping of cooling/heating branches below 250 K).

It is properly to mention that the area of the thermo-magnetic hysteresis inside the MT is field dependent. Increasing the field, the hysteresis area decreases and becomes zero at a given applied field. Increasing further the field the magnetization exhibits an augmentation during the cooling process and respectively, a diminution during the reverse process of heating, namely exactly an opposite behavior as compared to the case mentioned for low fields. One can say that the hysteresis changes the sign

and one can formally assign to the area of the loop, developed in higher fields, a corresponding negative sign. The specific behavior in high fields is related to a higher saturation magnetization of the martensite phase as compared to the austenite one [5], [20]. A similar abrupt variation of the magnetization, in the transformation temperature range, although not so pronounced, was observed also on the other samples, A0 and A1 [28]. Concluding the magnetic results, the Fe_{69.4}Pd_{30.6} alloy with FCC structure stabilized at room temperature, with T_C higher than MT temperature, is a FSMA.

4. Conclusions

High temperature stable FCC austenitic phase was quenched in Fe_{69.4}Pd_{30.6} ribbons and no irreversible transformation was found, only the first order and thermo-elastic martensitic transformation was highlighted via DSC and thermomagnetic measurements.

A proper thermal treatment of Fe_{69.4}Pd_{30.6} ribbons, at high temperature for short time, resulted in improved homogeneity and the crystalline structure was refined by stabilization of FCC phase. Alternatively, the annealing at low temperature promotes the reduction of the amount of transforming FCC phase by its partial decomposition in the stable phases.

The thermo-magnetic measurements performed at low magnetic field simulated a slow thermal treatment at higher temperatures, which allows to highlight the decomposition of the metastable FCC phase in two stable phases: BCC and L1₀. In addition, the field dependent thermo-magnetic hysteresis was identified, with opposite behavior for high and low magnetic fields.

In the further work is necessary to optimized the thermal treatments and the addition of the third alloying element, in order to induce the martensitic transformation at higher temperatures, so to stabilize the FCT structure at room temperature, behavior required by applications.

Acknowledgements

The authors thank PhD. M Valeanu for the useful discussions and PhD. M. Enculescu for assistance with the SEM facility. This work was supported by a grant of the Romanian Ministry of Research and Innovation, CCCDI - UEFISCDI, project number PN-III-P1-1.2-PCCDI-2017-0062 / contract no. 58/ component project no. 2, within PNCDI III.” and Core Program PN 18-110101.

References

- [1] R. Oshima, M. Sugiyama, *J. Phys. Colloq* **C4**, 383 (1982).
- [2] M. Matsui, K Adachi, *Physica B*, **161**, 53 (1989).
- [3] M. Matsui, J. P. Kuang, T. Totani, K. Adachi, *J. Magn. Magn. Mater.* **54-57**, 911(1986).
- [4] R. D. James, M. Wuttig, *Philos. Mag. A*, **77**, 1273 (1998).
- [5] J. Cui, T. W. Shield, R. D. James, *Acta Mater.* **52**, 35 (2004).
- [6] T. Wada, Y. Liang, H. Kato, T. Tagawa, M. Taya, T. Mori, *Mater. Science and Engineering A* **361**, 75 (2003).
- [7] K. Seki, H. Kura, T. Sato, T. Taniyama, *J. Appl. Phys.* **103**, 063910 (2008).
- [8] V. Sánchez-Alarcos, V. Recarte, J. I. Pérez-Landazábal, M. A. González, J. A. Rodríguez-Velamazán, *Acta Mater.* **57**, 4224 (2009).
- [9] C. D. Cirstea, F. Tolea, L. Leonat, M. Lungu, A. Cucos, V. Cirstea, V. Tsakiris, *J. Optoelectron. Adv. M.* **18** (9-10), 857 (2016).
- [10] C. Kavitha, M. G. Madhan, *J. Optoelectron. Adv. M.* **19**(11-12), 719 (2017).
- [11] C. Cosma, N. Balci, M. Moldovan, L. Morovic, P. Gogola, C. Miron-Borzan, *J. Optoelectron. Adv. M.* **19**(11-12), 738 (2017).
- [12] V. Sánchez-Alarcos, V. Recarte, J. I. Pérez-Landazábal, C. Gómez-Polo, V. A. Chernenko, M. A. González, *Eur. Phys. J. Special Topics* **158**, 107 (2008).
- [13] Y. C. Lin, C. F. Lin, J. B. Yang, H. T. Lee, *J. Appl. Phys.* **109**, 07A912 (2011).
- [14] D. Vokoun, C. T. Hu, *Scripta Mater.* **47**, 453 (2002).
- [15] F. Tolea, M. Tolea, M. Sofronie, M. Valeanu, *Solid State Communications* **213**, 37 (2015).
- [16] D. Vokoun, C. T. Hu, V. Kafka, *J. Magn. Magn. Mater.* **264**, 169 (2003).
- [17] C. T. Hu, T. Goryczka, D. Vokoun, *Scripta Mater.* **50**, 539 (2004).
- [18] D. Vokoun, T. Goryczka, C. T. Hu, *J. Alloys Compd.* **372**, 165 (2004).
- [19] R. Grossinger, R. Sato Turtelli, N. Mehmood, S. Heiss, H. Muller, C. Bormio-Nunes, *J. Magn. Magn. Mater.* **320**, 2457 (2008).
- [20] C. Bormio-Nunes, R. S. Tutelli, R. Grossinger, H. Muller, H. Sassik, *J. Magn. Magn. Mater.* **322**, 1605 (2010).
- [21] V. Recarte, C. Gómez-Polo, V. Sánchez-Alarcos, J. I. Pérez-Landazábal, *J. Magn. Magn. Mater.* **316**, e614 (2007).
- [22] R. Santamarta, A. Pasko, J. Pons, E. Cesari, P. Ochinnikov, *Mater. Trans.* **45**, 1811 (2004).
- [23] A. M. Glezer, E. N. Blinova, V. A. Pozdnyakov, A. V. Shelyakov, *J. Nanoparticle Research*, **5**, 551 (2003).
- [24] F. Tolea, G. Schinteie, B. Popescu, *J. Optoelectron. Adv. M.* **8**, 1502 (2006).
- [25] M. Sofronie, F. Tolea, V. Kuncser, M. Valeanu, *J. Appl. Phys.* **107**, 113905 (2010).
- [26] F. Tolea, M. Sofronie, C. Ghica, M. Valeanu, *Optoelectron. Adv. Mat.* **5**, 562 (2011).
- [27] T. Kakeshita, T. Terai, T. Fukuda, *J. Magn. Magn. Mater.* **321**, 769 (2009).
- [28] M. Sofronie, F. Tolea, V. Kuncser, M. Valeanu, G. Filoti, *IEEE Trans. Mag.* **51**, 2500404 (2015).

*Corresponding author: mihsof@infim.ro